Proceedings of the EuroGNC 2013, 2nd CEAS Specialist Conference
on Guidance, Navigation & Control, Delft University of Technology,
Delft, The Netherlands, April 10-12, 2013

Lateral Fly by Wire Control System dedicated to Future Small Aircraft

Matthias Heller[1], Thaddäus Baier[2] and Falko Schuck[3]

Institute of Flight System Dynamics (FSD) and Institute for Advanced Study (IAS), Technische Universität München (TUM), D-85748 Garching, Germany

Abstract. **Compared to common transport aircraft (airliners), it is fact that the General Aviation (GA) sector exhibits a significant higher rate of accidents. Even though the sources are manifold, two main reasons may be identified. First, General Aviation Pilots generally have a relative low training level and small number of flight hours compared to airliner pilots and thus, their flight experience and hazard awareness is consequently limited. The second reason is, that recent transport aircraft feature a significant higher technical standard possessing various beneficial pilot assistant systems supporting the pilot to fly the aircraft safely at the same time reducing pilot's workload extensively. The most vital assistant systems, well-known as Fly-by-Wire Flight Control Systems (FbW FCS), provide directly the appropriate control deflections according to the pilot's commands and (measured) flight condition and thus are capable to assume important safety enhancing tasks. In addition to ensuring excellent and homogenized flying/handling qualities along the whole envelope, they offer functionalities like pilot input monitoring, provision of warnings plus active envelope protection yielding a substantial increase of passenger, crew and aircraft safety towards the key objective "carefree handling". Unfortunately, this valuable safety increase did not find its way into the general aviation sector although it is standard in current transport planes and modern business jets. This is due to the tremendous cost of typical Fly-by-Wire control technology always requiring complex redundancy and reversionary systems to fulfill the strict certification requirements. However, in order to accomplish an equivalent safety enhancement for GA aircraft and thus to diminish the high accident rates and so to protect human lives, the well-proved beneficial features of active Flight Control Systems have to be made available and affordable for them.**

[1] Dr.-Ing. Matthias Heller, Rudolf Diesel Industry Fellow at TUM-IAS, Affiliate Professor at TUM, Email: matthias.heller@tum.de;
[2] Dipl.-Ing. Thaddäus Baier, Research Assistant, Email: th.baier@tum.de;
[3] Dipl.-Ing. Falko Schuck, Research Assistant, Email: schuck@tum.de;

An essential contribution to this subject is the major objective of the ambitious Technology Research Program "Future Small Aircraft (FSA)" of the Austrian aircraft manufacturer Diamond Aircraft Industries in cooperation with the Institute of Flight System Dynamics of the Technische Universität München. Within this joint multinational research program concerning upcoming Future Small Aircraft, (amongst others) the development of an appropriate FbW lateral flight control system is expedited. Although the control law design is primarily aimed for provision of excellent handling qualities and pilot's assistance, one main focus is also set on the elaboration of special processes, tools and hardware solutions enabling the progression of control algorithms which are perfectly tailored to the specific needs of manufacturers of small and medium-sized planes.

I. Introduction

By comparison of the accident statistics of General Aviation (GA) versus common transport aircraft (airliners) it becomes obvious that the General Aviation sector exhibits a significant higher rate of accidents (Ref. [8]). This fact is not new and even though the sources are manifold, two main reasons may be identified. On the one hand, General Aviation Pilots mostly hold a Private Pilot License (PPL) only and hence, their number of flight hours and thus their experience commonly is considerably limited in contrast to airliner pilots having an Airline Transport Pilot License (ATPL). On the other hand, current (modern) transport aircraft feature a noteworthy higher technical standard providing various beneficial pilot assistant systems in order to support the pilot to fly the aircraft safely and to reduce pilot's workload extensively.

The most important and effective assistant systems, which are well-known as Fly-by-Wire Flight Control Systems (FbW FCS) intervene directly and actively into the aircraft's control and besides improving and homogenizing flying and handling qualities considerably, they offer a wide range of functionalities including pilot input monitoring, provision of warnings plus limitations and advanced protections and hence, increase the passenger, crew and aircraft comfort and safety competently towards the overall ultimate objective "carefree handling".

This valuable increase in safety, which has become standard in current transport planes and modern business jets, unfortunately did not find its way into the general aviation sector due to the tremendous cost of typical Fly-by-Wire control technology always requiring complex redundancy and reversionary systems in order to fulfill the strict certification requirements and specifications. However, in order to achieve a corresponding safety enhancement for GA aircraft and hence to reduce the high accident rates and to protect human lives, the well-proved beneficial functionalities of active Flight Control Systems (active FCS) definitely have to be made available and affordable for them. Particularly, this holds in considera-

tion of the expected significant rise in the number of GA planes and movements (Ref. [10]), which otherwise would come along with a further increase in accidents and victims, which has to be avoided. Consequently, specifically tailored FbW FCS technology suitable and in particular affordable for GA airplanes has to be made available. For instance, recent accomplishments in the area of actuators, sensors and flight control computers (FCC) offer potential to design more cost-effective active assistance systems to be utilized within GA planes in the future.

A considerable contribution to this subject is one major objective of the ambitious Technology Research Program “Future Small Aircraft (FSA)” of the Austrian aircraft manufacturer Diamond Aircraft Industries in cooperation with the Institute of Flight System Dynamics of the Technische Universität München. Within this joint multinational Research program concerning upcoming Future Small Aircraft, first a hybrid control concept for longitudinal dynamics has been proposed, compare Ref. [7], which now is extended by the development of an appropriate lateral flight control system. Although the control law layout is aimed for provision of excellent homogeneous flying/handling qualities and pilots assistance, another main focus is set on the preparation of special processes, tools and hardware requirements/solutions supporting the design of control algorithms which are perfectly adapted to the specific needs of manufacturers of small and medium-sized planes.

Summarized, the development process applied comprises the following main issues:

– Elaboration of an universal controller structure for lateral dynamics which is suitable for all typical airplane configurations (fixed-wing aircraft with empennage) independent whether a full Fly-by-Wire or “Hybrid Flight Control System” will be applied, compare Ref. [7]
– Provision of a layout methodology denoted "Model Reference Direct Eigenstructure Assignment (*MR DEA*)" which is adapted to the controller structure in order to determine the gain sets/tables along the entire envelope
– Development of a tool for stability and robustness assessment incorporating a detailed uncertainty model which is suited for the controller structure proposed in order to facilitate the certification (e.g. μ-Analysis)

Testing of the whole development chain will be accomplished by implementing of the lateral controller developed into an appropriate general aviation aircraft simulator (DA-42 FTD) and finally, by actually flying it on the corresponding in-flight simulator "*Fliegender Erprobungsträger Bayern*", a research aircraft based on a DA-42 M-NG airframe planned and developed at the Institute of Flight System Dynamics of Technische Universität München.

II. Flight Dynamics Modeling

A small aircraft featuring an active Fly-by-Wire Flight Control System (FbW FCS) represents a new class of general aviation airplanes. By utilizing the benefits of such a system, some basic aircraft design objectives (e.g. static stability and damping characteristics) may be shifted to other focuses and thus, the aircraft concept may differ from today's conventional shape. Nevertheless, the novel FbW FCS must be implemented, demonstrated and tested within a suitable flying testbed before designing an entire new aircraft relying on such a novel FbW FCS. For this purpose, the Institute of Flight System Dynamics owns a fully-fledged Flight Control System Development and Integration Environment:

- An integrated tool chain to efficiently support Model Based Development (MBD) of functional algorithms for onboard applications. All tools used are compliant with airworthiness requirements.
- A DA-42 Flight Training Device (D-SIM42 FTD simulator) with extensive capability to simulate malfunctions of multiple aircraft systems for design and validation of control laws and pilot in the loop verification.
- A DA-42 Airframe and Control System Iron Bird for component tests and verification, integration tests for research aircraft and hardware in the loop simulation in connection with the Flight Training Device.
- And in particular a research aircraft Diamond DA-42 MPP NG (Multi Purpose Platform New Generation), particularly dedicated as in-flight simulator with an Experimental Fly-by-Wire (EFbW) control system, see Fig. 1.

Figure 1: Research Flying Testbed (DA-42 MNG) featuring EFbW FCS

With this continuous "end-to-end" development and integration chain at hand, it suggests itself to utilize the Diamond DA-42 aircraft as reference configuration. For this type of aircraft the feasibility, advantages and reliability of the active FbW FCS for general aviation aircraft will be analyzed, verified and finally (in-flight) demonstrated.

Regarding the functional layout and development of the control system, an appropriate high-fidelty flight simulator for functional testing is of vital importance. The available D-SIM42 Flight Training Device is equipped with original glass cockpit, *Garmin G1000 Avionics package* with primary flight display (*PFD*) as well as a multi-function display in order to achieve the most realistic cockpit envi-

ronment. The DA-42 simulator is thus a perfect tool for controller functionality pilot-in-the-loop testing under "real world" conditions. Unfortunately, the flight dynamics model as well as all internal signal processing are completely capsuled "black boxes" and entirely isolated from external inputs. Both is adverse for an application of the simulator as design and implementation platform for the active FCS to be developed.

For this reason, an new nonlinear six 6 dof model called "FSD DA-42/FSA 6 DOF Flight Dynamics & Simulation Model" has been implemented using *MATLAB / Simulink* and its top-level block structure is shown in Fig. 2. Particular emphasis was placed on a high fidelity physical modeling and on a exact reproduction of the dynamics of the D-SIM42 FTD simulator.

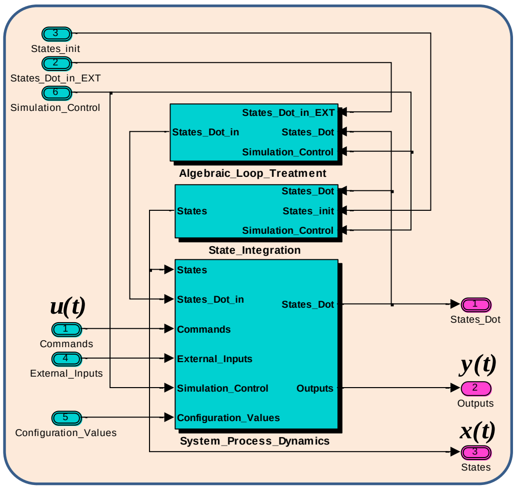

Figure 2: FSD DA-42/FSA Nonlinear 6 DOF Flight Dynamics & Simulation Model

The validation of the FSD DA-42/FSA 6 DOF flight dynamics model was accomplished by systematic simulator flight tests conducted in the D-SIM42 device as detailed within Ref. [7] assuring an adequate matching versus the D-SIM42 FTD.

III. Lateral Controller Design

Objectives, derived Requirements, deduced "Design Philosophy"

The main objective of the FSA lateral control design is to provide excellent flying/handling qualities along the entire envelope in order to reduce pilot's workload significantly when flying the airplane manually. Related objectives are to increase

the safety and comfort of passengers and crew together with the efficiency of the aircraft (fuel consumption).

To achieve these goals, it is required to improve and homogenize the stability and command characteristics to keep them intuitive and predictable over the operational envelope and to accomplish an effective gust load rejection. Additionally the effects of configuration changes shall automatically be compensated and a further reduction of the pilot's workload shall be achieved by partial automation of secondary controls, e.g. spoiler or thrust setting.

Consequently, the following primary design objectives may be deduced and committed in terms of our "design philosophy":

- Modification of the aircraft's stability characteristics:
  The basic stability characteristics and thus the flying qualities, shall be modified by assignment of "optimal" damping, frequency and time constants to the different eigenmodi of the lateral motion.
- Augmentation of the command behavior:
  - Rate Command/Attitude Hold (*RC*/*AH*) versus angle of sideslip (*AOS*) Command/zero lateral load characteristics:
    The provision of velocity vector roll and angle of sideslip command has shown to be very intuitive and predictable for the pilot in combination with attitude hold or zero lateral load factor characteristics respectively when the inceptor is released.
  - Feed Forward Path Augmentation:
    By implementation of a "direct link" feed forward branch, it is possible to improve the aircraft's control sensitivity and to cancel out the integrator poles of the corresponding command transfer function n order to obtain a more "crisp" control behavior
- Decoupling of control inputs (introduction of decoupled "auxiliary control effectors"):
  To manually fly a velocity vector roll, the pilot would have to apply coordinating rudder command and vice versa a pure buildup of sideslip would require adding adequate aileron deflections to the pedal command. This maneuver coordination for the decoupling of experimental roll and yaw axes shall be accomplished automatically by means of auxiliary control inputs. A respective control axes decoupling is not only convenient for the pilot, it also makes the subsequent controller layout much more intuitive and straightforward.
- Counteracting external disturbances (gusts/turbulence) and compensating for changes of the aircraft configuration:
  External disturbances shall be suppressed efficiently as well as changes in the configuration (e.g. by deflecting the wing flaps, by a malfunction of an engine or by extending and retracting the landing gear) shall be compensated as far as possible in order to further reduce the pilot's workload.

Controller Structure

As described within the previous section, the controller to be developed has to comply with several different objectives. The specific design goals are thereby typically associated with the different branches in the controller structure. Subsequently, the overall controller structure as depicted in Fig. 3 is introduced and the design philosophy is detailed by discussion of every branch.

Generally, the controller consists of the *Command Signal Generation* providing roll rate and angle of sideslip commands, decoupling *Yaw* and *Roll Axis Controller* relying on the calculated commands and sensor feedbacks creating generalized input variables that correspond to a demanded roll and yaw control moment w.r.t. the experimental-axis, respectively as well as the *Control Allocation* converting the generalized input variables to equivalent allocated control surface deflection commands.

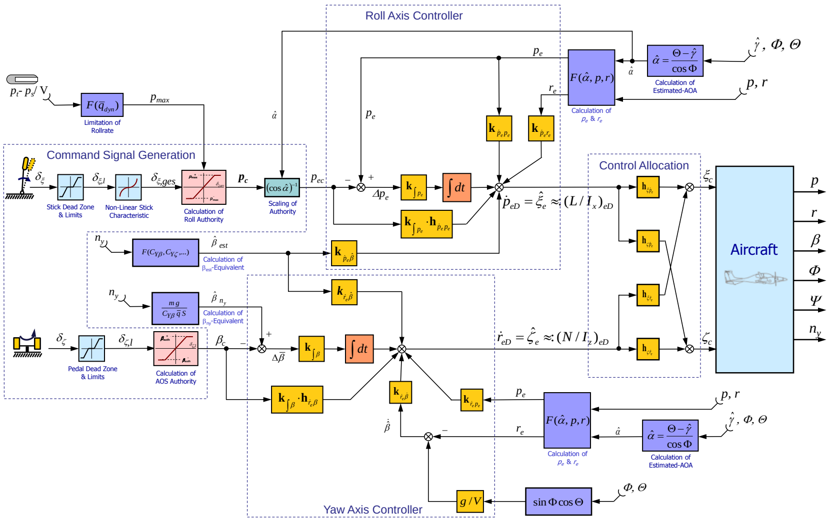

Figure 3: Controller Structure

To ensure proper function of the controller, high and low frequency measurements have to be available appropriately, as listed in the following table (whereas the “hat-variables” represent not directly measured but estimated signals).

High Frequency Measurements	*Low Frequency Measurements*
$n_y,\ p,\ r$	$\Phi,\ \Theta,\ (\hat{\gamma})$

Table 1: Measurement Signals

- ***Control Allocation ("Decoupled virtual controls")***
  As previously stated, the aircraft shall roll around the velocity vector and yaw around the experimental *z*-axis (generating a pure $\dot{\beta}$) for improved command behavior and easier controllability (decoupling of roll and yaw motion) and thus, to increase flight efficiency.

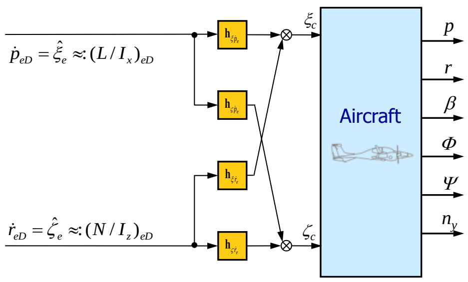

Figure 4: Control Allocation (Subfigure to Figure 3)

With such an approach, using a ("reversionary") direct link law a lateral stick input of the pilot (*roll rate command*) yields only a roll acceleration ($\dot{p}_e$) around the aerodynamic flow direction without any excitation of the angle of sideslip. Conversely, a pedal input (*angle of sideslip command*) would introduce a pure yaw rate (r_e) without any excursion of the bank angle, i.e. the aircraft does not tilt to the side like a typical unaugmented aircraft.

To achieve such decoupled virtual controls, the lateral control surfaces (aileron and rudder) need to be coordinated in such a manner, that a roll rate command generates a pure moment around the x_e-axis. Accordingly, an angle of sideslip command has to produce a pure moment around the z_e-axis.

Eqn. (1) provides the linear state space model of the lateral motion w.r.t. experimental axes. Via the entries N_ξ and L_ζ in the input matrix $\boldsymbol{B}$, an aileron deflection ξ results in an adverse rotational (yaw) acceleration ($\dot{r}_e$) and a rudder deflection (ζ) results in an undesired rotational (roll) acceleration $\dot{p}_e$, respectively.

$$\dot{\boldsymbol{x}} = \boldsymbol{A}\,\boldsymbol{x} + \boldsymbol{B}\,\boldsymbol{u} \quad \Leftrightarrow \quad \begin{pmatrix} \dot{p}_e \\ \dot{r}_e \\ \dot{\beta} \\ \dot{\Phi} \end{pmatrix} = \begin{bmatrix} L_p & L_r & L_\beta & 0 \\ N_p & N_r & N_\beta & 0 \\ Y_p & Y_r - 1 & Y_\beta & \frac{g_0}{V_0}\cos\Theta_0 \\ \frac{\cos\gamma_0}{\cos\Theta_0} & \frac{\sin\gamma_0}{\cos\Theta_0} & 0 & 0 \end{bmatrix} \cdot \begin{pmatrix} p_e \\ r_e \\ \beta \\ \Phi \end{pmatrix} + \begin{bmatrix} L_\xi & L_\zeta \\ N_\xi & N_\zeta \\ Y_\xi & Y_\zeta \\ 0 & 0 \end{bmatrix} \cdot \begin{pmatrix} \xi \\ \zeta \end{pmatrix} \tag{1}$$

The necessary feed forward law for *control allocation* in order to decouple the control axes may be derived from the desired change of states due to the control surface deflections:

$$\begin{pmatrix} \dot{p}_{eD} \\ \dot{r}_{eD} \end{pmatrix} = \begin{bmatrix} L_\xi & L_\zeta \\ N_\xi & N_\zeta \end{bmatrix} \cdot \begin{pmatrix} \xi \\ \zeta \end{pmatrix} =: \begin{pmatrix} \hat{\xi}_e \\ \hat{\zeta}_e \end{pmatrix} \tag{2}$$

Eqn. (2) introduces the virtual "auxiliary" control surfaces $\hat{\xi}_e$ and $\hat{\zeta}_e$ which act directly on the x_e respectively z_e-axis. Inversion of Eq. (2) provides a suitable feed forward control law:

$$\begin{pmatrix}\xi\\ \zeta\end{pmatrix}=\begin{bmatrix}h_{\xi\dot{p}_e} & h_{\zeta\dot{p}_e}\\ h_{\xi\dot{r}_e} & h_{\zeta\dot{r}_e}\end{bmatrix}\cdot\begin{pmatrix}\dot{p}_{eD}\\ \dot{r}_{eD}\end{pmatrix}\qquad \text{with}\qquad \begin{bmatrix}h_{\xi\dot{p}_e} & h_{\zeta\dot{p}_e}\\ h_{\xi\dot{r}_e} & h_{\zeta\dot{r}_e}\end{bmatrix}=\begin{bmatrix}L_\xi & L_\zeta\\ N_\xi & N_\zeta\end{bmatrix}^{-1} \tag{3}$$

Substitution of (ξ, ζ) in the state space model (1) by the control allocation law Eq. (3) yields the dynamics augmented by decoupled "auxiliary" control inputs as suitable basis for the subsequent controller layout:

$$\begin{pmatrix}\dot{p}_e\\ \dot{r}_e\\ \dot{\beta}\\ \dot{\Phi}\end{pmatrix}=\begin{bmatrix}L_p & L_r & L_\beta & 0\\ N_p & N_r & N_\beta & 0\\ Y_p & Y_r-1 & Y_\beta & \frac{g_0}{V_0}\cos\Theta_0\\ \frac{\cos\gamma_0}{\cos\Theta_0} & \frac{\sin\gamma_0}{\cos\Theta_0} & 0 & 0\end{bmatrix}\cdot\begin{pmatrix}p_e\\ r_e\\ \beta\\ \Phi\end{pmatrix}+\underbrace{\begin{bmatrix}1 & 0\\ 0 & 1\\ \breve{Y}_\xi & \breve{Y}_\zeta\\ 0 & 0\end{bmatrix}}_{\breve{B}}\cdot\begin{pmatrix}\hat{\xi}_e\\ \hat{\zeta}_e\end{pmatrix} \tag{4}$$

Nevertheless, as may be seen from Eq. (4) the virtual "auxiliary" controls still exhibit undesired side-effects on the $\dot{\beta}$-equation due to the application of a partial inversion of the input matrix $\boldsymbol{B}$. However, via analytical as well as numerical analyses it could be verified, that the magnitudes of the residual derivatives $\breve{Y}_\xi, \breve{Y}_\zeta$ are negligible compared to the other contributions of the side-force equation, compare Table 2. Hence, for the succeeding controller design they can be set to zero as it was subsequently justified within the "Controller Analysis" without neglected side-force residuals, see Chapter V.

	DA 42 (Cruise) [Source: Simulation Model FSD]		Do 328 (Cruise) [Data extracted from Ref. [4]]
	110kts	90kts	
$\breve{Y}_\xi=\frac{Y_\xi N_\zeta - Y_\zeta N_\xi}{L_\xi N_\zeta - L_\zeta N_\xi}$	$-7.49\cdot10^{-4}$	-0.00170	$9.205\cdot10^{-4}$
$\breve{Y}_\zeta=\frac{-Y_\xi L_\zeta + Y_\zeta L_\xi}{L_\xi N_\zeta - L_\zeta N_\xi}$	-0.0120	-0.0179	-0.0150

Table 2: Example Values of $\breve{Y}_\xi$ and $\breve{Y}_\zeta$

Remark: Alternatively, a corresponding feed forward control allocation law may be introduced by means of the *Moore-Penrose Pseudo-Inverse* of the control matrix $\boldsymbol{B}$. However, it could be shown, that the results of both methods are almost identical within the numerical accuracy.

- ***Command Signal Generation***
  The Command Signal Generation path scales and limits the stick and pedal deflections appropriately and provides predictable and intuitive stick/pedal characteristics to the pilot. Subsequently, an authority calculation in terms of the maximum commanded roll rate and angle of sideslip according to the airworthiness limitations is performed depending on the current flight condition.

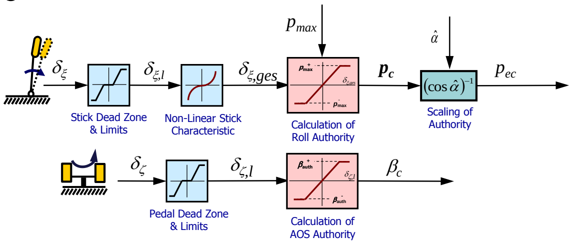

Figure 5: Command Signal Generation (Subfigure to Figure 3)

- ***Roll Axis Controller***
  After introduction of the decoupled "virtual controls" (see previous section) the roll axis controller basically represents a classical *PI*-scheme augmented by a direct link path in order to ensure the desired RC/AH characteristic, see Fig. 6.
  Here, the integrator path ensures zero steady-state error w.r.t. the commanded roll rate. The direct link path on the other hand is used to improve the roll command behavior (initial reaction) of the aircraft w.r.t. excellent handling qualities by "cancelling" out the integrator pole of the stick-to-roll transfer function. Via the gains $k_{\dot{p}_e r_e}$ and $k_{\dot{p}_e \beta}$, the yaw axis cross coupling on the roll axis will be eliminated. The specific layout of the roll controller gains is detailed within next section "*Model Reference Direct Eigenstructure Assignment*".

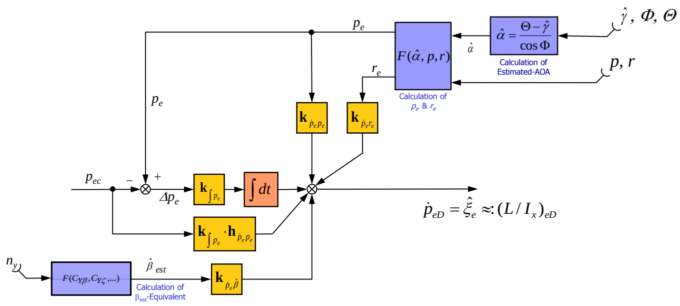

Figure 6: Roll Axis Controller (Subfigure to Figure 3)

- ***Yaw Axis Controller***
  Correspondingly, based on the control decoupling functionality (see previous section), the yaw axis controller consists of an analogous *PI*-structure augmented by a direct link path in order to modify the damping

and natural frequency of the dutch roll and to shape adequate command characteristics, see Fig. 7.
Again, the integrator path ensures steady-state accuracy with regard to the commanded angle of sideslip (AoS) versus the n_y equivalent AoS signal denoted β_{ny} in Figs. 5 and 7. Again, the feed-forward (direct link) branch is introduced to improve the command behavior of the aircraft in terms of excellent handling qualities by "cancelling out" the integrator pole. Via the gain $k_{\dot{r}_e p_e}$ the main cross coupling from the roll to the yaw axis will be compensated.

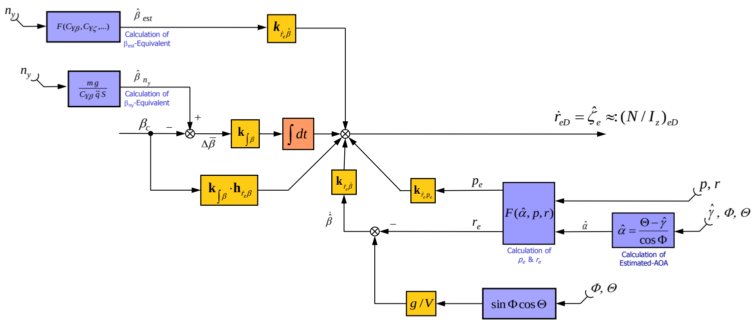

Figure 7: Yaw Axis Controller (Subfigure to Figure 3)

- ***Estimated and Equivalent Flow Angle Signals***

Due to the fact, that General Aviation/small aircraft commonly do not feature a sideslip and/or an angle of attack vane/sensor, there is generally no applicable measurement of the angle of sideslip and/or the angle of attack (AoA) available and for flight control purposes they have to be estimated conveniently. An appropriate subsidiary signal for (measured) AoS which can be used for sideslip feedback may be calculated as follows (Ref. [9]):

$$\hat{\beta}_{est} = \left(\frac{m\, g\, n_{ye}}{\bar{q}\, S} - C_{Q\zeta}\, \zeta - C_{Qr}\, r - C_{Qp}\, p \right) \frac{1}{-C_w + C_{Q\beta}} \tag{5}$$

Currently, the necessary aerodynamic derivatives for the AoS estimation in Eq. (5) are taken from the aerodynamic model within the simulator. However, in future it is intended to validate or (if applicable) substitute them via flight test parameter identification.
Similarly, the angle of attack signal utilized by the controller is generated by the simple, but well-proven relationship (Ref. [9]):

$$\hat{\alpha} = \frac{\Theta - \hat{\gamma}}{\cos\Phi} \tag{6}$$

In contrast to the roll axis branch, where the controller uses only one feedback signal (roll rate p_e), the yaw axis controller applies two different feedback signals: $\hat{\beta}_{est}$ and $\hat{\beta}_{n_y}$. Here, $\hat{\beta}_{n_y}$ represents a scaled equivalent sideslip signal proportional to the lateral load factor which is defined as:

$$\hat{\beta}_{n_y} = \frac{m\, g\, n_{ye}}{\bar{q}\, S\, C_{Q\beta}} \tag{7}$$

The use of $\hat{\beta}_{n_y}$ for the integral feedback path (in addition to $\hat{\beta}_{est}$ for proportional feedback) is motivated by a desired zero side force flight condition ($n_y = 0$) in case of zero pedal (i.e. $\beta_c = 0$). If the aerodynamic AoS or the corresponding estimated $\hat{\beta}_{est}$ (acc. to Eqn. (5)) would be utilized for integral feedback, even in straight and level flight a small residual side force would remain ($n_y \neq 0$) due to unavoidable minor asymmetric effects (e.g. propulsion, lateral c.g. shift, asymmetric aerodynamics) and hence, a sustained yaw/turn rate and consequently drift would occur. On the other hand, applying an n_y-equivalent integral feedback acc. to Eq. (7) signal always ensures zero side force in (zero pedal) steady state condition und thus, a well-coordinated flight without any drift.

Model Reference Direct Eigenstructure Assignment (MR DEA)

An intuitive and preserving full visibility approach for the layout of the specific controller gains (feedback, feedforward plus cross-feed), which is directly suited to assure excellent flying qualities has been elaborated and is proposed here referred to as "Model Reference Direct Eigenstructure Assignment (*MR DEA*)".

The basis for the calculation of the controller gains is formed by the state space model of the closed loop system with the control allocation in terms of "decoupled virtual controls" applied as introduced before. Concerning the linear gain layout, the differences between real and estimated AoS, i.e. β, $\hat{\beta}_{est}$ and $\hat{\beta}_{n_y}$ are negligible and hence, are not taken into account and the unified feedback signal is β. However, the validity of this assumption has to be proved within the controller analysis and (nonlinear) assessment, which could have been accomplished successfully.

First, the control allocation gains ($h_{\xi \dot{p}_e}$, $h_{\zeta \dot{p}_e}$, $h_{\xi \dot{r}_e}$, $h_{\zeta \dot{r}_e}$) are calculated as given by Eqn. (3). Next, based on the introduction of the "decoupled virtual controls" (see Fig. 3) the closed loop state space model (including the two integrator states $x_{\int \Delta p}$, $x_{\int \Delta \beta}$) with the side force residuals $\breve{Y}_\xi$, $\breve{Y}_\zeta$ set to zero can be evaluated to:

$$
\begin{pmatrix} \dot{r}_e \\ \dot{\beta} \\ \dot{p}_e \\ \dot{\Phi} \\ \dot{x}_{\int \Delta p} \\ \dot{x}_{\int \Delta\beta} \end{pmatrix}
=
\begin{bmatrix}
N_r - k_{\dot{r}_e\dot{\beta}} & N_\beta + k_{\dot{r}_e\hat{\beta}} & N_p + k_{\dot{r}_e\dot{p}_e} & k_{\dot{r}_e\dot{\beta}}\dfrac{g_0}{V_0}\cos\Theta_0 & 0 & k_{\int\beta} \\
Y_r - 1 & Y_\beta & Y_p & \dfrac{g_0}{V_0}\cos\Theta_0 & 0 & 0 \\
L_r + k_{\dot{p}_e\dot{r}_e} & L_\beta + k_{\dot{p}_e\hat{\beta}} & L_p + k_{\dot{p}_e p_e} & 0 & k_{\int p_e} & 0 \\
\dfrac{\sin\gamma_0}{\cos\Theta_0} & 0 & \dfrac{\cos\gamma_0}{\cos\Theta_0} & 0 & 0 & 0 \\
0 & 0 & 1 & 0 & 0 & 0 \\
0 & 1 & 0 & 0 & 0 & 0
\end{bmatrix}
\cdot
\begin{pmatrix} r_e \\ \beta \\ p_e \\ \Phi \\ x_{\int \Delta p} \\ x_{\int \Delta\beta} \end{pmatrix}
+
\begin{bmatrix}
0 & k_{\int\beta} h_{\dot{r}_e\beta} \\
0 & 0 \\
k_{\int p_e} h_{\dot{p}_e p_e} & 0 \\
0 & 0 \\
-1 & 0 \\
0 & -1
\end{bmatrix}
\cdot
\begin{pmatrix} p_{ec} \\ \beta_c \end{pmatrix}
\tag{8}
$$

Fig. 8 depicts the closed-loop system matrix $\boldsymbol{A}_{CL}$ with the decisive subsystems and specific elements highlighted according to their significance w.r.t. the (desired) closed-loop dynamics and the controller gain layout as further explained below.

Initially, in order to provide a proper "best possible" decoupling of the roll and the yaw (control) axis, the dedicated controller cross feed gains of elements (boxes) number 1, 2 and 3 each are adjusted to cancel the corresponding entry out, i.e. to make the coupling element equal to zero. The closed-loop derivative number 6, which represents a special case of controller induced coupling will be discussed later separately.

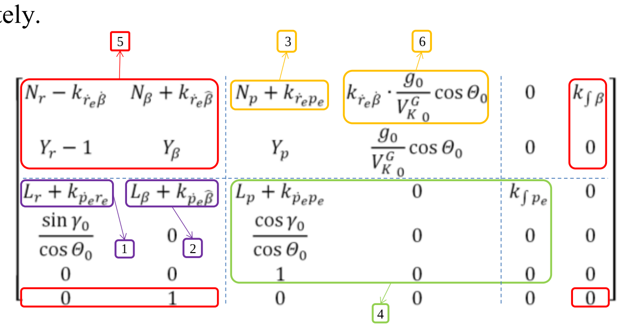

Figure 8: Closed Loop System Matrix

After application of this pre-decoupling and omitting the remaining coupling elements in the closed-loop system matrix $\boldsymbol{A}_{CL}$ (due to the fact that they are small and hence, with minor impact on the dynamics as will be verified in Chapter IV), two almost decoupled subsystems are achieved with corresponding dynamic matrices $\boldsymbol{A}_{\boldsymbol{R}}$ and $\boldsymbol{A}_{\boldsymbol{Y}}$ of roll and yaw axis, respectively (green box #4 and red boxes # 5 in Fig. 8):

$$\boldsymbol{A}_R = \begin{bmatrix} L_p + k_{\dot{p}_e p_e} & 0 & k_{\int p_e} \\ \dfrac{\cos\gamma_0}{\cos\Theta_0} & 0 & 0 \\ 1 & 0 & 0 \end{bmatrix} \qquad \boldsymbol{A}_Y = \begin{bmatrix} N_r - k_{\dot{r}_e \dot{\beta}} & N_\beta + k_{\dot{r}_e \hat{\beta}} & k_{\int \beta} \\ Y_r - 1 & Y_\beta & 0 \\ 0 & 1 & 0 \end{bmatrix} \tag{9}$$

The desired closed-loop (reference) dynamics of the roll and yawing motion (including the controller introduced integrator poles) are each represented by their characteristic polynomials. Regarding the roll axis we specify

$$N_{CL,R}(s) = (T_{R,d}\, s + 1)(T_{IR,d} s + 1) s = (T_{R,d}\, T_{IR,d} s^2 + (T_{R,d} + T_{IR,d}) s + 1) s \tag{10}$$

where T_{R,d_D} is the desired roll time constant, $T_{IR,d}$ the desired integrator time constant and the free "s" represents the neutrally stable spiral mode according to the aspired RC/AH characteristics.

Similarly, for the yaw channel the reference characteristic polynomial is:

$$\begin{aligned} N_{CL,Y}(s) &= (s^2 + 2\zeta_{DR,d}\, \omega_{0DR,d}\, s + \omega_{0DR,d}^2)(T_{IY,d} s + 1) \\ &= T_{IY,d}\, s^3 + (2\zeta_{DR,d}\, \omega_{0DR,d}\, T_{IY,d} + 1) s^2 + (2\zeta_{DR,d}\, \omega_{0DR,d} + T_{IY,d} \omega_{0DR,d}^2) s + \omega_{0DR,d}^2 \end{aligned} \tag{11}$$

with the desired dutch roll damping $\zeta_{DR,d}$, frequency $\omega_{0DR,d}$ and the integrator time constant $T_{IY,d}$, respectively.

By calculation of the corresponding characteristic polynomials of the closed-loop subsystem matrices in Eq. (10) and coefficient comparison with Eqs. (11, 12) the basic feedback gains $(k_{\dot{p}_e p_e}, k_{\int p_e}, k_{\dot{r}_e \dot{\beta}}, k_{\dot{r}_e \hat{\beta}}, k_{\int \beta})$ can be determined successively in order to achieve the desired stability characteristics (in terms of closed-loop roll time constant, dutch roll damping and frequency) which are assigned according to the so-called MIL Level 1* specifications (Ref. [1-3]) (i.e. middle of Level 1 boundary).

For a typical open loop dynamics or a pure yaw rate feedback the controller induced cross coupling element (# 6 in Fig. 8) is zero. However, in order to provide a suitable turn coordination and thus, to improve the handling qualities effectively, an elegant measure is to remove the steady turn yaw rate $\sin\Phi \cos\Theta\, g / V$ from the measured (over all) yaw rate feedback signal (see Fig. 3, in fact an equivalent sideslip time-derivative will be fed back here). This yields the artificial cross coupling (#6 in Fig. 8) which supports a well coordinated flight without sideslip excitations or deviations when turning/banking.

Finally, the feed-forward gains of the two direct link paths (Figs. 6 & 7) may assigned straight-forward via the corresponding closed-loop transfer functions for roll rate and sideslip. From Eq. (9) the transfer functions $g_{p_e p_{ec}}(s)$ and $g_{\beta\beta_c}(s)$ may be easily derived (e.g. applying the *Cramer* rule) as :

$$g_{p_e p_{ec}} = \frac{k_{\int p_e} h_{\dot{p}_e p_e} (s - 1/h_{\dot{p}_e p_e})}{(s+1/T_R)(s+1/T_{IR})} \text{ , where } k_{\int p_e} = -1/(T_R T_{IR}) \tag{12}$$

$$g_{\beta\beta_c} = \frac{k_{\int \beta} h_{\dot{r}_e \beta} (Y_r - 1)(s - 1/h_{\dot{r}_e \beta})}{(s^2 + 2\zeta_{DR}\omega_{0DR} s + \omega_{0DR}^2)(s+1/T_{IY})} \text{ , where } k_{\int \beta} = \omega_{0DR}^2/(T_{IY}(1-Y_r)) \tag{13}$$

Here the design objective is an crisp "typical aircraft-like" initial response (without perceiving the integrator lags) and hence, the feed-forward gains $h_{\dot{p}_e p_{ec}}$ and $h_{\dot{r}_e \beta}$ each are computed to cancel out the corresponding integrator pole in the denominator polynomial, i.e. $h_{\dot{p}_e p_e} = -T_{IR}$, $h_{\dot{r}_e \beta} = -T_{IY}$.

A great advantage of the design methodology presented is, that based on the in-depth system knowledge in terms of the structure of the (closed-loop) system matrices ($\boldsymbol{A}_{CL}$, $\boldsymbol{B}_{CL}$) and the correlation with most favorable flying qualities (acc. to the so-called MIL Level 1* specifications (Ref. [1-3])) the controller gains can be determined straight-forward without any iteration in order to ensure the assigned reference dynamics (compare Ref. [5]). In contrast, classical direct eigenstructure assignment e.g. requires a numerical method to compute the feedback gain matrix $\boldsymbol{K}$ with the quality of solution (achieved eigenstructure) is strongly depending on a careful specification of desired (attainable) eigenvalue/eigenvector sets (nullspace projection) and the assignability of single controller gains to specific flying quality requirements is almost lost (e.g. Ref. [6]).

IV. Controller Analysis

In order to verify the controller design philosophy and to demonstrate the capability of the approach proposed an extensive controller assessment has been performed. As a first step, a linear controller and robustness analysis is accomplished by calculation of the closed loop eigenvalues and eigenvectors, linear simulations (e.g. step responses) and classical *SISO* (single input single output) nichols plots (simultaneous gain/phase margins for rudder an aileron cuts).

Fig. 9 depicts the open-loop, the desired and the closed loop-poles (eigenvalues) for a representative flight condition of the DA-42 with V_{TAS} = 139 kts, h =916.3 m, m = 1590 kg and an intermediate c.g. position x_{CG} = -2.3727 m (mean design point).

Generally, the resulting closed-loop poles match the assigned desired locations very well. Merely the closed loop dutch roll oscillation a shows a perceptible offset compared to the specified "ideal" location featuring a relative error in natural frequency ω_{0DR} about 0.5 % and an error in relative damping of 0.025 %. However, these deviations are really small and can be proven to depend on the intentionally neglected coupling derivatives (as Y_p) and side force residuals ($\breve{Y}_\xi, \breve{Y}_\zeta$) within

the layout procedure. Moreover, they act in a conservative way (higher damping) and hence, are regarded to be (fully) acceptable.

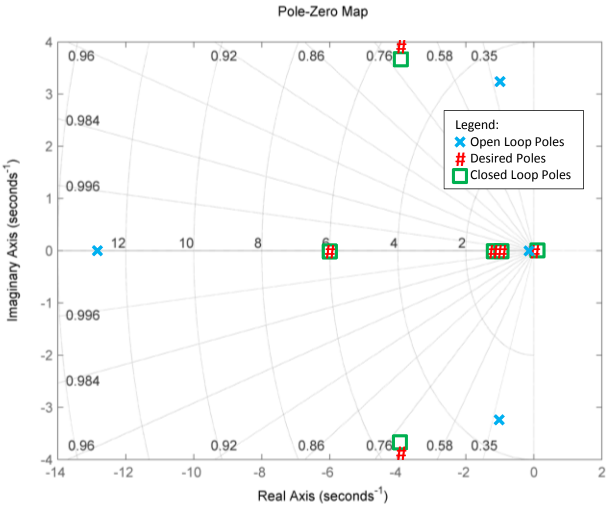

Figure 9: Open-Loop / Desired / Closed Loop Poles (Eigenvalues)

The best way to illustrate the capability of the *MR DEA* design procedure applied may yield the comparison of the open-loop, the "ideal" reference and the resulting closed-loop dynamics in terms of the corresponding system matrices $\boldsymbol{A}$, see Fig. 8 and Table 3. The light grey shadowed elements represent the controller decoupling effects and the dark grey highlighted entry embodies the artificial cross coupling supporting a well coordinated flight without sideslip excitations ("turn compensation") as discussed above. As may bee seen from Table 3 in comparison with Fig. 8 the decoupling capability of the control scheme presented is very effective and the aspired structure revealing two decoupled subsystems for roll and yaw channel could be achieved quite fairly.

States	Open Loop $\boldsymbol{A}$-Matrix				Closed Loop $\boldsymbol{A}$-Matrix					
r_e	-1.8764	10.1548	-0.4523	0.0000	-8.5759	36.0948	0	0.9185	0	30.2855
β	-0.9988	-0.2341	0.0054	0.1371	-0.9337	-0.4908	-0.0004	0.1282	0.0014	-0.2933
p_e	1.0826	-22.9306	-12.8038	-0.0000	0	0	-7.0000	-0.0000	-6.0000	0
Φ	0	-0.0000	1.0001	0.0000	0	-0.0000	1.0001	0.0000	0	0
$x_{\int \Delta p}$	-	-	-	-	0	0	1.0000	0	0	0
$x_{\int \Delta \beta}$	-	-	-	-	0	1.0000	0	0	0	0

Table 3: Open- and Closed-Loop A-Matrix

The excellent decoupling potential is further highlighted by the computation of the associated open-loop versus the closed-loop eigenvectors, see Tables 4 and 5. The adverse entries concerning the states p_e and Φ within the dutch roll eigenvec-

tor vanish and conversely, the undesirable effects of p_e and especially β are cancelled out in the spiral eigenvector.

Open – L o o p			
States	Dutch Roll	Roll Mode	Spiral Mode
r_e	0.8359	-0.0379	0.1312
β	0.0630 $\pm$ 0.2473i	-0.0034	0.0226
p_e	-0.1656 $\pm$ 0.4357i	-0.9963	-0.0294
Φ	-0.1077 $\pm$ 0.0851i	0.0776	0.9907

Table 4: eigenvectors open loop

C l o s e d – L o o p					
States	Dutch Roll	Roll Mode	Spiral Mode	Yaw Int. Dyna.	Roll Int. Dyna.
r_e	0.9833	0.0111	-0.1336	-0.5342	-0.0160
β	0.1248 $\pm$ 0.1286i	0.0057	-0.0000	-0.6061	-0.1111
p_e	-0.0000 $\pm$ 0.0000i	0.9733	0.0000	0.0000	-0.5701
Φ	0.0000 $\pm$ 0.0000i	-0.1622	-0.9910	-0.0000	0.5701
$x_{\int\Delta p}$	0.0000 $\pm$ 0.0000i	-0.1622	0.0000	-0.0000	0.5701
$x_{\int\Delta\beta}$	-0.0008 $\pm$ 0.0327i	-0.0010	-0.0078	0.5892	0.1110

Table 5: eigenvectors closed loop

Summarizing, the *MR DEA* approach proposed provides an effective means for excellence in flying quality design in terms of directly assigning a desired reference dynamics to the closed-loop system matrices based on an in-depth knowledge of their shape (structure and settings) in order to meet typical ideal "Level 1" flying quality requirements.

In a second step, the linear design has been verified successfully by repetition of the controller analysis (as presented above) after integration of the flow angle estimations plus necessary filters (i.e. n_y-noise filter, etc.), sensor and actuator models along the entire envelope plus a subsequent *SISO* robustness prove by means of Nichols plots (sufficient phase and gain margins).

V. Nonlinear Simulation Results (Controller Assessment)

With the primary intention to demonstrate (i.e. to fly) the controller and its capabilities in flight on our Research Flying Testbed (DA-42 MNG), the designed lateral control system has been appropriately discretized and implemented within the DA-42 FTD simulator to perform a comprehensive (nonlinear) assessment including simulator flight test to gain pilot evaluation/ratings.

Initially, single axis square inputs of pedal and lateral stick are applied to validate the functionality (especially the command and decoupling behavior) of the nonlinear flight control system implementation. Fig. 10 shows the closed-loop response to a β_C = 5 deg pedal input (duration 8 sec) for the DA-42 representative reference flight condition as specified before (V_{TAS} = 139 kts, h =916.3 m, c.g. position x_{CG} = -2.3727 m, m = 1590 kg). It should be noted (as detailed within Chapter III) that the integrator feedback signal is a scaled equivalent sideslip $\hat{\beta}_{n_y}$ proportional to the lateral load factor and hence, this signal reveals the typical all-pass behavior, initially to the wrong side due to the rudder side force opposite to the final $C_{Y\beta}\,\beta$. Moreover, the $\hat{\beta}_{n_y}$ -integrator in conjunction with the decoupling design ensures steady-state accuracy without any bank angle and restores zero lateral load factor after pedal release guaranteeing a coordinated flight (n_y=0).

Accordingly, in Fig. 11 the time histories of a p_C = 10 deg/sec square wave input (duration 2 sec, then 4 sec zero input followed by 2 sec opposite square) for the same reference flight condition are depicted. Correspondingly, the p_e-integrator provides zero steady-state error and the *MR DEA* approach in combination with the pre-decoupling "virtual controls" yield well coordinated aileron and rudder deflections assuring a pure velocity vector roll without significant (equivalent) sideslip excitation.

Currently, the controller gains are fixed and it could be shown that with such a set an acceptable behavior in terms of flying/handling qualities along the whole envelope can be achieved. However, in a next step, the control system layout will be enhanced by a straightforward gain-scheduling depending on calibrated airspeed involving a strictly limited number of grid points as preliminary investigations raise expectations that about 3 to 5 interpolation points are quite sufficient.

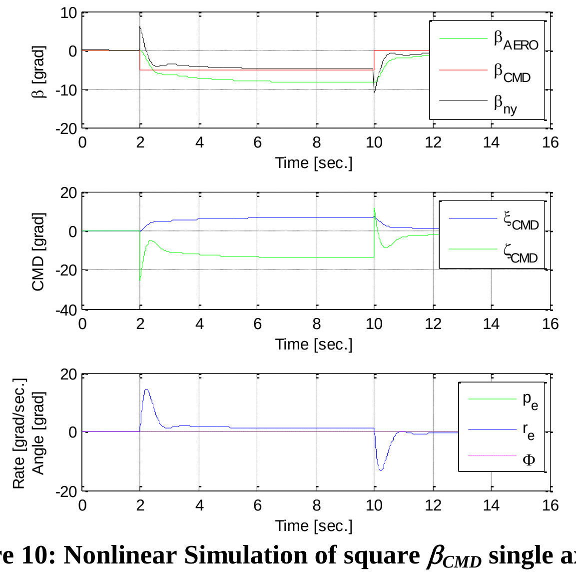

Figure 10: Nonlinear Simulation of square β_{CMD} single axis input

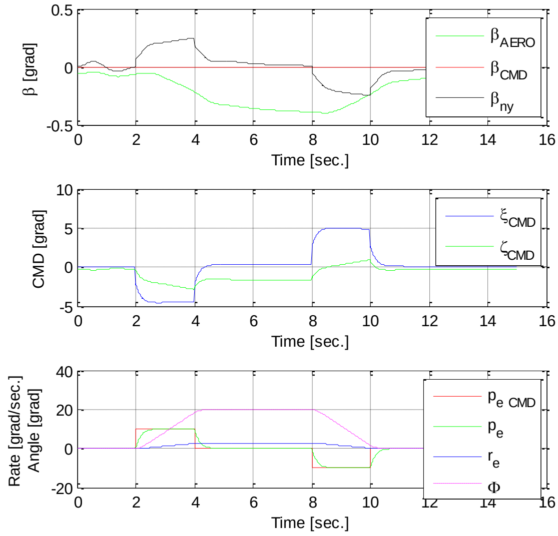

Figure 11: Nonlinear Simulation of square p_{CMD} single axis Input

VI. Conclusions

The development of a novel Fly-by-Wire Control System for the augmentation of the lateral dynamics, specifically tailored to future small general aviation aircraft is presented. This control system provides excellent flying qualities and pilot assistance under special regard of the cost-benefit ratio (i.e. acceptable engineering, implementation and certification efforts).

The unique requirements and constraints posed by the introduction of an advanced active Flight Control System into small aircraft such as *a priori* limited (by rate and position) actuator deflections or the compliance with general aviation typical sensor equipment, are addressed. Besides an appropriate feasible structural layout according to the particular needs of such a low cost/low complexity but high reliability flight control system, the feedforward and feedback gain design w.r.t. relevant flying and handling qualities criteria and its interactions are considered. Additionally, the complete development chain ranging from the nonlinear flight dynamics engineering model via the general aviation aircraft simulator up to the in-flight simulator DA-42 NG available at the Institute of Flight System Dynamics of Technische Universität München is presented.

It can be demonstrated, that current state of the art benefits of modern Fly-by-Wire technology may be provided by the active lateral Flight Control System considered by simultaneously observing the objectives and limitations specified. The control system design is confirmed by recent simulator flight tests which reveal not only a significant flying and handling qualities improvement attaining high pilot's acceptance. Additionally, the safety and assistance functionalities like turn compensation, velocity vector roll and command decoupling as well as bank angle

protection excellently fulfill the pilot's demand for effective safety increase and assistance under manual control.

Consequently, the next steps after some modifications and fine tunings due extensive simulator flight tests are represented by systematic pilot testing plus evaluation and subsequently, a comprehensive stability and robustness assessment (linear as well as nonlinear) will be performed. Amongst others, this includes on the one hand a *SISO* robustness analysis based on Nichols charts (single loop cuts) which supports and facilitates the certification process. Additionally, a detailed uncertainty model will be elaborated as fundamental basis for the overall *MIMO* robustness prove (μ-Analysis) ensuring robust stability and performance along the entire envelope with special regard to typical real-word system delays and parametric as well as dynamic uncertainties.

Acknowledgments This paper was prepared with the support of the Technische Universität München - Institute for Advanced Study, funded by the German Excellence Initiative.

References

[1]Department of Defense, MIL-STD-1797, Military Standard, "Flying Qualities of Piloted Vehicles", Washington, 1995

[2]Department of Defense, MIL-F-8785C, Military Specification, "Flying Qualities of Piloted Airplanes", Washington, 1980

[3]Department of Defense, MIL-HDBK-1797, Military Standard Handbook, "Flying Qualities of Piloted Vehicles – Handbook", Washington, 1997

[4]Brockhaus, R., "*Flugregelung*"; Springer-Verlag, Berlin Heidelberg New York, 1996, 2. Edition

[5]Garrard, William L., "Lateral Directional Aircraft Control Using Eigenstructure Assignment", Journal of Guidance, Control, and Dynamics, Vol. 21, No. 3, 1998, pp. 523-525

[6]Heller, M., "Untersuchung zur Steuerung und Robusten Regelung der Seitenbewegung von Hyperschall-Flugzeugen", Herbert Utz Verlag, Muenchen, 1999

[7]Heller, M., Schuck, F., Peter, L., Holzapfel, F., " Hybrid Control System for a Future Small Aircraft", AIAA Guidance, Navigation, and Control Conference, Portland, Oregon, Aug. 2011, AIAA-2011-6635

[8]Emma, K., "Australia probes high fatal accident rate in GA sector", Flight International, Reed Business Information Ltd., 19-25 July 2011, Page 21,

[9]Heller, M., Myschik, S., Holzapfel, F., Sachs, G., "Low-cost Approach based on Navigation Data for Determining Angle of Attack and Sideslip for Small Aircraft" AIAA Guidance, Navigation, and Control Conference and Exhibit, Austin, TX, Aug. 2003, AIAA-2003-5777

[10]U.S. Department of Transportation - Federal Aviation Administration - Aviation Policy and Plans, "FAA Aerospace Forecast Fiscal Years 2010-2030", [pdf Document online], available at: https://www.faa.gov/data_research/aviation/aerospace_forecasts/2010-2030/ [22.01.2013]